July, 2004

Effects of Simulated Flash Fire and Variations in Skin Model on Manikin Fire Test

Guowen Song, *North Carolina State University*
R. Barker, *North Carolina State University*
D. Thompson, *North Carolina State University*
R. Grimes, *North Carolina State University*

Journal of ASTM International, July/August 2004, Vol. 1, No. 7
Paper ID JAI12116
Available online at www.astm.org

Guowen Song,[1] *R. Barker,*[2] *D. Thompson,*[2] *and R. Grimes*[2]

Effects of Simulated Flash Fire and Variations in Skin Model on Manikin Fire Test

---

ABSTRACT: An established numerical model of a manikin fire test, which has the capability of predicting heat transfer through thermally protective clothing exposed to an intense heat environment, is described in this paper. The model considers the fire characteristics simulated in a manikin chamber as well as the insulating air layers between protective garments and the skin surface. The numerical model is applied to analyze the effects of simulated flash fire and variations in a skin model on a manikin test. The study demonstrates that the heat flux measured by 122 thermal sensors over the surface of the manikin exhibits a bell-shaped Gaussian distribution for a short duration in calibration burn. A series of flash fire data with different distributions was generated statistically, and the effects on burn predictions were investigated. The results suggest that the fire distribution affects the burn predictions for 4 s of exposure. The effects of initial temperature distribution, thermal properties, as well as involvement of blood perfusion in a skin model on burn predictions are also discussed. The model predictions demonstrate that the initial temperature distribution in a skin model has a large effect on burn predictions for a one-layer garment exposed to short duration flash fire conditions.

KEYWORDS: skin model, flash fire, manikin fire test, fire distribution, thermal protective performance, temperature distribution, blood perfusion

Introduction

An instrumented manikin fire testing system is the most realistic laboratory assessment of the thermal protective performance of garments or ensembles. This manikin fire test system can control heat flux; flame distribution; duration; garment size, fit, and style; as well as the physical constitution of the wearer. Environmental conditions can be assessed in addition to the garment materials. This life-size thermal burn evaluation system is the fastest, most reproducible, and most advanced measurement system in the world today.

Figure 1 illustrates the basic elements of the Pyroman® [1] fire testing and burn evaluation processes. Laboratory flash fire is generated in the Pyroman® burn chamber by eight propane-burning torches. The heat from the fire transfers through the fabric and through the air gap between the protective garment and the manikin body. The temperatures are registered by 122 heat flux sensors on the manikin body. Predictions of skin burn injury resulting from the flash fire exposure are made using a skin model. The test procedure, data acquisition, result calculations, and test report preparation are performed with computer hardware and software programs.

Manuscript received 18 November 2003; accepted for publication 13 May 2004; published July/August 2004. Presented at ASTM Symposium on Performance of Protective Clothing: Global Needs and Emerging Markets: 8th Symposium on 13 January 2004 in Tampa, FL.

[1] Research Associate, Center for Research on Textile Protection and Comfort, College of Textiles, North Carolina State University, Raleigh, NC.
[2] Professor, Associate Director, and Special Project Director, respectively, College of Textiles, North Carolina State University, Raleigh, NC.

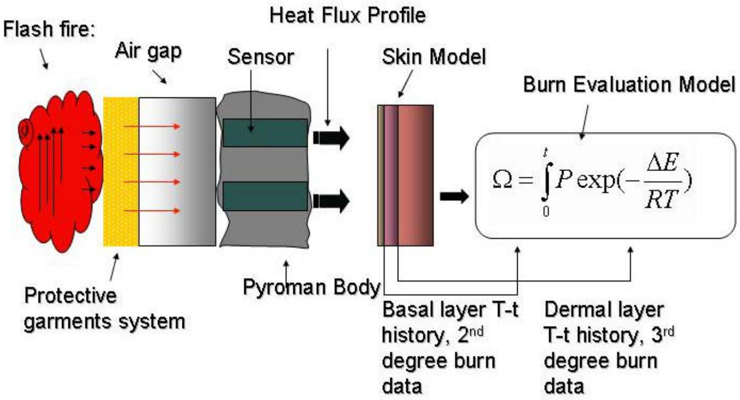

FIG. 1—*Heat transfer in instrumented manikin fire testing system.*

The flash fire generated in the Pyroman® chamber is by turbulent jet flames generated by eight propane torches around the manikin body. In the calibration process, the simulated flash fire is adjusted to produce an overall heat flux of 2.0 cal/cm^2·s for 4 s of exposure. The overall heat flux is an average heat flux measured by the 122 thermal sensors distributed over the manikin. The measured heat fluxes by the 122 sensors are not uniform because of the dynamic nature of the flame column surrounding the manikin and the complexity of human body geometry. The measured heat fluxes are then applied to a skin model programmed in the computer to calculate the temperature-time history in the skin layers. With this temperature-time history, burn injury predictions are made based on Henriques Burn Integral [2].

The literature proposes different skin models for human skin exposed to thermal hazards [3–5]. They differ in layer structure, layer thermal properties, initial temperature distribution, and blood perfusion. The simulated flash fire in the manikin chamber can produce different fire distributions but maintain an average heat flux of 2.0 cal/cm^2·s. In this paper an established numerical model of the manikin fire testing was used to examine the effect of fire distribution and variations in the skin model on manikin burn predictions for one-layer garments.

Numerical Model of Manikin Fire Testing

The model used by this research considers the entire burning process based on 122 sensor locations (Fig. 2). Heat transfer through the fabric and air layers is computed in conduction, radiation, and convection modes. A heat transfer equation is applied in conjunction with a skin model to estimate the temperature profile in the basal and dermal layers of the skin. Our model assumes that convective heat transfer occurs only at the surface of the protective fabric. Radiative heat flux is assumed to penetrate the fabric only to a certain depth. Based on these assumptions, the energy balance in a fabric element is [6]:

$$\rho_{fab}(T) Cp_{fab}(T) \frac{\partial T}{\partial t} = \frac{\partial}{\partial x}\left(k_{fab}(T) \frac{\partial T}{\partial x} \right) - \gamma \cdot q_{rad} e^{-\gamma x} \tag{1}$$

where ρ_{fab} is the density of the fabric; Cp_{fab} is the specific heat; k_{fab} is the thermal conductivity; and γ is the extinction coefficient of the fabric determined from transmissivity and the fabric thickness. The incident radiation (q_{rad}) can be expressed as:

$$q_{rad} = \sigma\varepsilon_g(T_g^4 - T_{fab}^4) - \sigma\varepsilon_{fab}F_{fab-amb}(1-\varepsilon_g)(T_{fab}^4 - T_{amb}^4) \qquad (2)$$

where σ is the Stefan-Boltzmann constant; ε_g, and ε_{fab} are the emissivity of the hot gases and the fabric, respectively; T_g, T_{fab}, and T_{amb} are the temperatures of the hot gases, the outside surface of the fabric, and the ambient air, respectively; and $F_{fab\text{-}amb}$ is the view factor which accounts for the geometry of the fabric in relation to the ambient air.

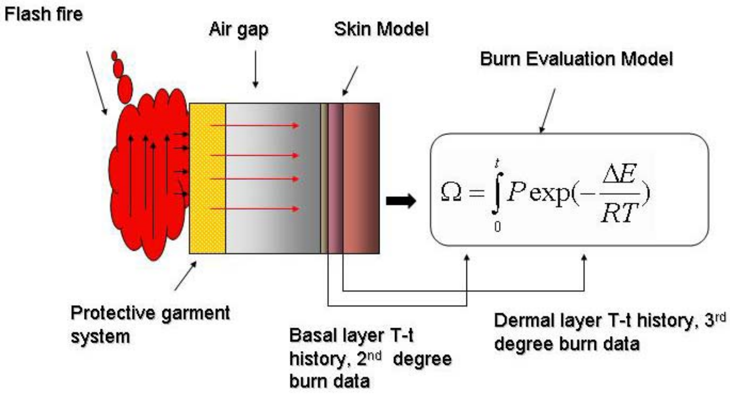

FIG. 2—*Elements of fabric air-gap skin model.*

The experimental foundation for the model was provided by three distinct experimental studies. The first experimental study characterized the thermal boundary conditions associated with the complex fire environment surrounding the manikin clothed in test garments. The second experimental base provided a means of estimating changes in the thermal physical properties of protective clothing material resulting from intense heat exposure. The third experimental analysis quantified the insulating air layers in skin-clothing systems and the changes in air gap distribution over the clothed manikin body due to garment shrinkage.

Flame temperatures measured over Pyroman® in the fire chamber ranged from 800–1400°C in a 4 s exposure to 2.0 cal/cm^2·s heat. The intensity of the incident thermal energy is normally distributed over the Pyroman® body. Variations in the incident heat flux result from the three-dimensional shape of the manikin surface and the complex and dynamic nature of the flame column surrounding the manikin. In order to compute heat transfer from the fire to the manikin, an overall heat transfer coefficient was estimated at each of the 122 thermal sensor locations [7].

Fabric thermal conductivity and heat capacity are the main factors controlling heat transfer in fabrics. The manikin model used a parameter estimation approach to quantify changes in fabric properties that occur as a result of intense heat exposure [8]. Experiments were conducted to estimate heat induced changes in the thermal conductivity and volumetric heat capacity of Kevlar®/PBI and Nomex®ШA fabrics in short duration (4 s) intense fire exposures. The results show that both thermal conductivity and volumetric heat capacity decrease during the exposure [9].

The air trapped between the protective garment and the body is a major factor determining thermal protective insulation. Three-dimensional body scanning technology was used to measure the air gap distribution that exists between different size protective garments and the manikin body [9]. The process used data which were taken from a dressed manikin superimposed on data taken from an unclothed manikin.

The skin can be modeled as a three-layer structure composed of an avascular epidermis, a highly-perfused dermis, and a poorly-perfused subcutaneous tissue. In the three-layer structure skin model, different thermal properties are used in epidermis, dermis, and subcutaneous tissue [11]. Within each layer the tissue properties are assumed to be homogeneous, isotropic, and of uniform thickness. Pennes' Model was adopted to describe heat transfer in human skin. The bio-heat transfer equation [10] is written as:

$$\rho_s c_{p_s} \frac{\partial T}{\partial t} = \nabla \cdot (k_s \nabla T) + (\rho c_p)_b \omega_b (T_a - T) \tag{3}$$

where ρ_s and $c_{p,s}$ are the density and specific heat of human tissue; k_s is the thermal conductivity of human skin; ρ_b and $c_{p,b}$ are the density and the specific heat of the blood; ω_b is blood perfusion factor (0.00125 $m^3/s/m^3$); and T_a is arterial blood temperature.

The numerical model was validated using a Pyroman® manikin dressed in Kevlar®/PBI and Nomex®IIIA coveralls with exposure times from 3–4 s (Fig. 3). Results from the numerical model successfully correlate with experimental Pyroman® results for one-layer Kevlar®/PBI and Nomex®IIIA protective coveralls exposed for short intervals [9].

Numerical Model Predictions

Simulated Flash Fire in Manikin Chamber

The Pyroman® flash fire exposure was characterized by measuring the flame temperature and corresponding heat flux along each of the 122 sensors distributed over the manikin body. Figure 4 shows the distribution of heat flux values of the 122 sensors in Pyroman®, illustrating a bell-shaped distribution. In order to access this distribution normality further, a normal scores plot was performed, which demonstrated that the heat flux distribution with an average of 2.0 $cal/cm^2 \cdot s$ during a 4 s exposure exhibits an approximate normal distribution. Variations in heat fluxes are expected due to the three-dimensional shape of the manikin surface and because of the complex and dynamic nature of the flame column surrounding the manikin. Therefore, depending on the location on the manikin body (e.g., arms, legs, shoulders), sensors located in different positions on the manikin body will have different heat flux values with respect to the flash fire.

In the manikin test, an average heat flux of 2.0 $cal/cm^2 \cdot s$ measured from the 122 sensors on the manikin is used to simulate flash fire conditions, and the standard deviation of these heat flux distributions is between 0.25–0.5. Figure 5 shows the bell-shaped distributions with a different standard deviation. The larger standard deviation indicates that more extreme high and low flux values occurred during the exposure. In order to examine the effects of different fire distributions, a series of heat flux data with different distributions was generated to simulate statistically the different fire distributions. These data, as a model fire boundary input, were predicted with a one-layer garment using the numerical model. The model is based on one-layer Kevlar®/PBI coverall. The major parameters used in the numerical model are described in Table 1. Figure 6 outlines the model calculations.

The standard deviation of the heat fluxes of all 122 Pyroman® sensors predicted by this model does not show a significant influence on third-degree burn prediction. The second-degree burn prediction, however, decreases as the standard deviation increases, as illustrated in Fig. 6. This is expected; as the standard deviation increases, more low heat flux values are generated.

This lowered heat flux value could help reduce the burn predictions. For 3 s of exposure, no significant difference was predicted on the results of second-degree burn.

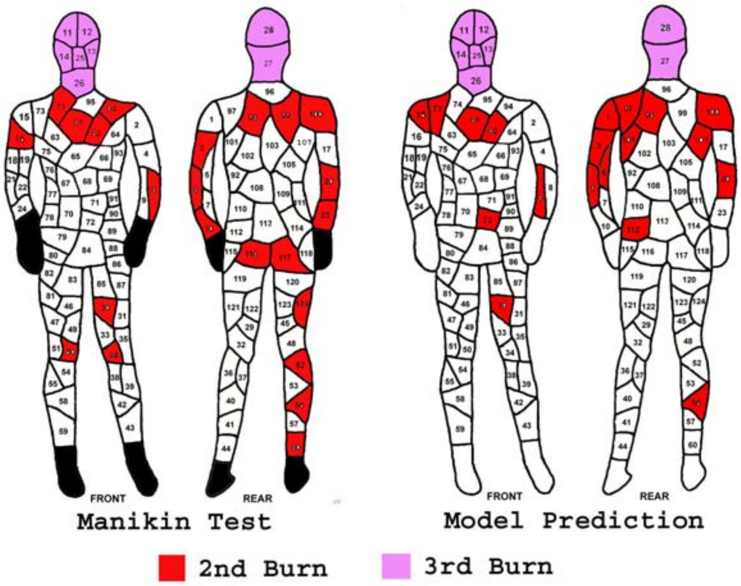

FIG. 3—*A comparison of burn distribution from manikin test and model prediction for 3 s exposures.*

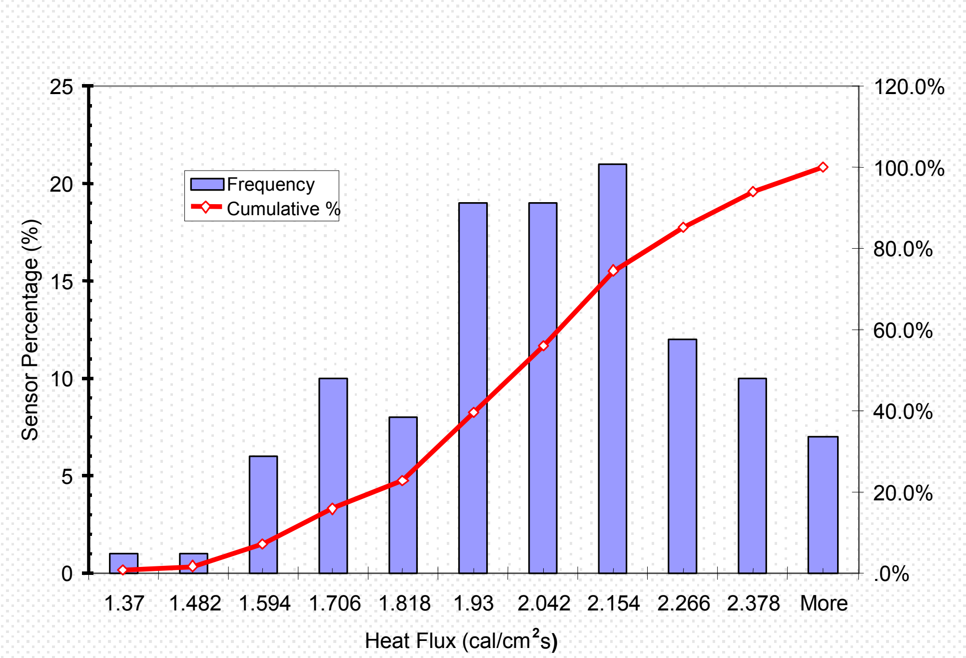

FIG. 4—*Histogram and cumulative curve of heat fluxes of 122 sensors over the manikin in 4 s exposures.*

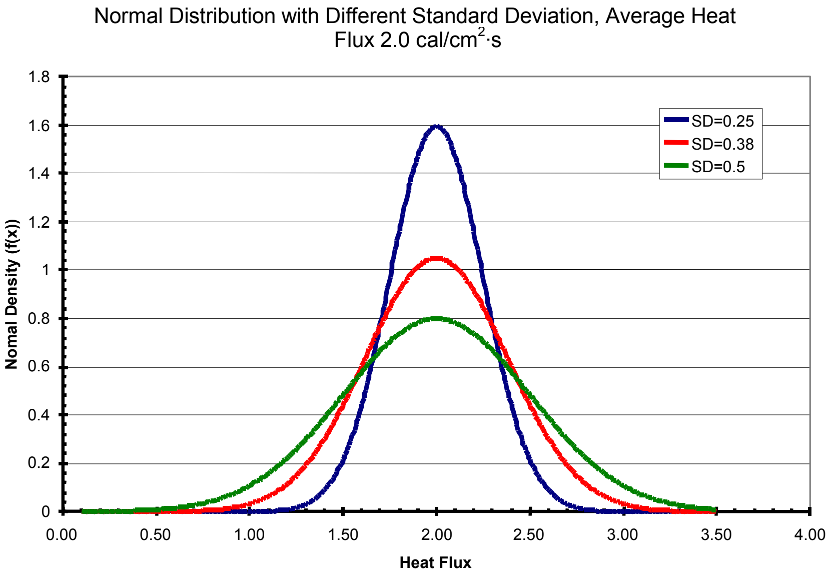

FIG. 5—*Heat flux distribution with different standard deviation.*

TABLE 1—*Parameters used in numerical model.*

Model Parameters	Value
Average Heat Flux	2.00 cal/cm^2·s
Fabric Weight	153g/m^2
Garment Air Gap Sizes	Kevlar®/PBI Coverall size 42 [9]
Garment Size	42
Burning Time (s)	3 or 4

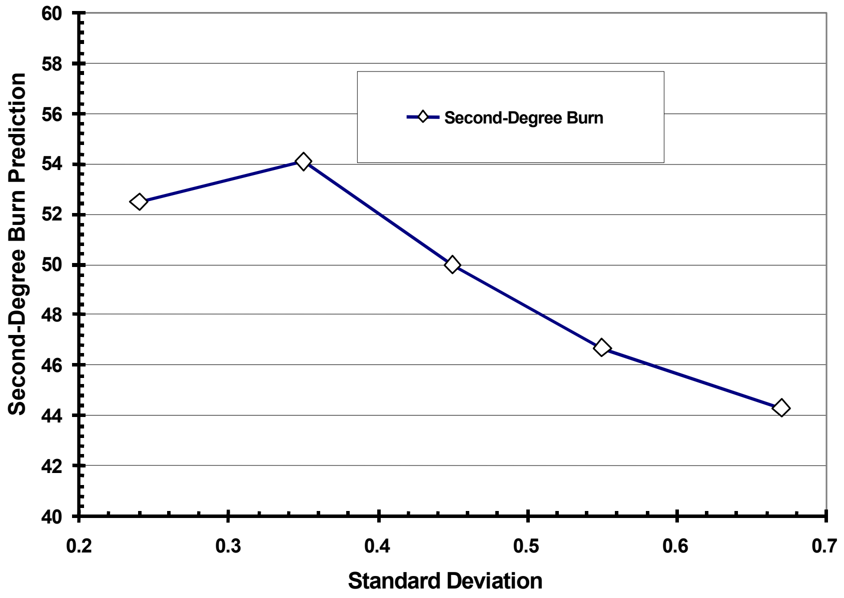

FIG. 6—*One-layer coverall manikin fire testing predictions with different fire distribution (overall average heat flux is 2.0 cal/cm^2·s).*

Skin Model

The variations in the skin model were analyzed using the manikin numerical model based on a one-layer coverall (Table 1). Table 2 summarizes the thermal physical properties used in one-layer and three-layer skin models [11].

Skin Temperature Distribution—One of the functions of human skin is to help regulate the body's core temperature. The core temperature of the body must be maintained within a small range around 37°C in order to keep biochemical reactions proceeding at required rates. Under normal ambient conditions, the skin surface temperature is about 32.5°C–34°C. Some skin models proposed constant initial skin temperatures of 32.5°C [12], 34°C [13], or 37°C [14]. Some other models suggest linear initial or higher order initial temperature distribution. For a given incident heat flux history transmitted through the garment under a flash fire condition, different initial temperature distribution in a skin model could affect the temperature rising rate at specific depth in the skin. In this study, five initial temperature distributions are selected. The first three are constant at 32.5, 34, and 37°C from surface to subcutaneous base; the fourth is a linear distribution from 32.5°C surface to 37°C subcutaneous; and the fifth is a quadratic distribution from 32.5°C surface to 37°C subcutaneous base. Temperature distributions in the different skin models are also examined. The one-layer skin model was constructed using properties shown in Table 2. The model prediction results are illustrated in Tables 3 and 4.

TABLE 2—*Thermal properties in different skin models.*

Properties	One-Layer	Three-layer [11]		
	Tissue	Epidermis	Dermis	Subcutaneous
Thermal Conductivity (W/m°C)	0.335	0.225	0.523	0.167
Volumetric Heat Capacity ($J/m^3 \cdot K*10^6$)	3.87	4.32	3.87	2.76

TABLE 3—*Temperature distribution effects in three-layer skin model in a 4 s exposure.*

Burn Prediction	Constant at 32.5°C	Constant at 34°C	Constant at 37°C	Linear from 32.5 to 37°C	Quadratic from 32.5 to 37°C
Second %	43.44	52.46	77.05	44.26	49.18
Third %	7.38	8.2	9.84	7.38	8.2
Total (%)	50.82	60.66	86.89	51.64	57.38

TABLE 4—*Temperature distribution effects in one-layer skin model in a 4 s exposure.*

Burn Prediction	Constant at 32.5°C	Constant at 34°C	Constant at 37°C	Linear from 32.5 to 37°C	Quadratic from 32.5 to 37°C
Second %	73.77	74.5	73.77	74.59	74.59
Third %	6.56	6.56	7.38	6.56	6.56
Total (%)	80.33	81.06	81.15	81.15	81.15

In the three-layer skin model, the predictions are very sensitive to initial temperature distributions. The linear and quadratic temperature distributions show almost a 10 % difference in burn predictions, while the constant temperature (37°C) distribution compared to the linear and quadratic indicates a large influence on second body burn prediction. The changes of these temperature distributions show little influence on third-degree burns. This result is expected because the temperature difference of these three distributions is very small at the interface of dermis and subcutaneous. In the one-layer skin model, however, initial temperature distribution shows little effect on burn predictions. The simulation results demonstrate that the burn predictions on initial temperature distribution in the one-layer skin model are not as sensitive as in the three-layer skin model. This result is attributable to the relative large thermal conductivity used in the one-layer skin model.

Blood Perfusion—A simulation was performed to determine the influence of the blood perfusion in the skin model on burn predictions in flash fire conditions. Two different blood perfusion values [9] were used in the skin model with comparison to the model without blood perfusion. The numerical results lead us to believe that blood perfusion in the skin model shows no effect on burn predictions in short duration flash fire conditions. Blood perfusion does not practically influence the burn prediction in terms of second and third body burns for the short exposure. However, as shown in Table 6, it changes the time to second- or third-degree burn at some specific individual sensor locations, especially when the prediction time is relatively longer. The time change is anticipated because the longer time allows the blood an opportunity to carry away some of the energy before damage is sustained.

TABLE 5—*Blood perfusion influence on burn predictions.*

	$G = 0$ ($m^3/s/m^3$)		$G = 1.25 \times 10^{-3}$ ($m^3/s/m^3$)		$G = 2.5 \times 10^{-3}$ ($m^3/s/m^3$)	
Sensor No.	Time to Second Burn (s)	Time to Third Burn (s)	Time to Second Burn (s)	Time to Third Burn (s)	Time to Second Burn (s)	Time to Third Burn (s)
3	2.27	12.3	2.27	12.45	2.27	12.55
20	2.62	14.2	2.62	14.45	2.62	14.75
85	6.61	no	6.62	no	6.63	no
92	7.16	no	7.19	no	7.61	no

Conclusion

The results of the numerical model predictions demonstrate that a different fire distribution in manikin fire testing exhibits influence on second burn predictions for a one-layer garment in a 4 s exposure. For a 3 s exposure, however, no significant difference is found on burn predictions. In addition, a decreased trend of prediction is found when the standard deviation increases. The results suggest that both the overall average heat flux and the precise standard deviation of a simulated flash fire should be indicated in order to enhance the manikin prediction.

Assuming blood perfusion in a skin model has minimal effect on predicted body burns in these exposures. The model assuming blood perfusion slightly increases the time to second- or third-degree burns, especially when the time to get second- or third-degree burns exceeds 5 s.

Different temperature distributions in the skin models demonstrate a large effect on burn predictions in the three-layer skin model. The effect is pronounced in the constant temperature distribution compared to linear and quadratic. In the one-layer skin model, however, initial temperature distribution shows little effect on burn predictions. Large second-degree burn predictions are observed in the one-layer skin model relative to the three-layer skin model. This study suggests that the use of different skin models and their initial temperature distributions can greatly affect burn predictions of garment testing in an instrumented manikin. Therefore, a precise skin model selection and its standardization would be beneficial for manikin testing in thermal protective performance evaluation.

References

[1] Pawar, M., and Barker, R. L., "Analyzing the Performance of Protective Garments in Manikin Fire Tests," *Proceedings of the Fifth Scandinavian Symposium on Protective Clothing*, Elsinore, Denmark, 1997.

[2] Henriques, F. C. and Moritz, A. R., "Studies of Thermal Injury: The Conduction of Heat to and Through Skin and the Temperatures Attained Therein. A Theoretical and Experimental Investigation," *American Journal of Pathology*, Vol. 23, 1947, p. 531.

[3] Buettner, K., "Effects of Extreme Heat and Cold on Human Skin II. Surface Temperature, Pain and Heat Conductivity in Experiments with Radiant Heat," *Journal of Applied Physiology*, Vol. 3, 1951, pp. 703–713.

[4] Mehta, A. K., and Wong, F., "Measurement of Flammability and Burn Potential of Fabrics," *Summary Report from Fuels Research Laboratory*, Massachusetts Institute of Technology, Cambridge, Massachusetts, 1972.

[5] Weaver, J. A., and Stoll, A. M., "Mathematical Model of Skin Exposed to Thermal Radiation," *Aerospace Medicine*, Vol. 40, 1969, pp. 24–30.

[6] Torvi, D. A., "Heat Transfer in Thin Fibrous Materials Under High Heat Flux Conditions," Doctoral Thesis, University of Alberta, Canada, 1997.

[7] Beck, J. V., Blackwell, B., and St. Clair, C. R., Jr., "Inverse Heat Conduction: Ill-Posed Problems," John Wiley & Sons, Inc., New York, 1985.

[8] Beck, J. V. and Arnold, K., "Parameter Estimation in Engineering and Science," Wiley, New York, 1977.

[9] Song, G., "Modeling Thermal Protection Outfits for Fire Exposures," Doctoral Dissertation, North Carolina State University, Raleigh, NC, 2002.

[10] Pennes, H. H., "Analysis of Tissue and Arterial Blood Temperatures in Resting Human Forearm," *Journal of Applied Physiology*, Vol. 1, 1948, pp. 93–122.

[11] ASTM F 1930-00: Standard Test Method for Evaluation of Flame Resistant Clothing for Protection Against Flash Fire Simulations Using an Instrumented Manikin, *Annual Book of ASTM Standards*, Vol. 11, No. 3, ASTM International, West Conshohocken, PA, 2003.

[12] Stoll, A. M., and Greene, L. C., "Relationship Between Pain and Tissue Damage Due to Thermal Radiation," *Journal of Applied Physiology*, Vol. 14, 1959, pp. 373–382.

[13] Diller, K. R., and Hayes, I. J., "A Finite Element Model of Burn Injury in Blood Perfused Skin," *Transactions of the ASME, Journal of Biomechanical Engineering*, Vol. 105, 1983, pp. 300–307.

[14] Henriques, F. C., Jr., "Studies of Thermal Injuries V. The Predictability and the Significance of Thermally Induced Rate Process Leading to Irreversible Epidermal Injury," *Archives of Pathology*, Vol. 43, 1947, pp. 489–502.